Controlling the Growth Mechanism of ZnO Nanowires by Selecting Catalysts

Z. Zhang

School of Physical and Mathematical Sciences, Nanyang Technological University, 1 Nanyang Walk, Singapore 637616, Singapore

S. J. Wang

Institute of Materials Research and Engineering, 3 Research Link, Singapore 117602, Singapore

T. Yu and T. Wu*

School of Physical and Mathematical Sciences, Nanyang Technological University, 1 Nanyang Walk, Singapore 637616, Singapore

Received: July 7, 2007; In Final Form: September 17, 2007

The effect of catalysts on ZnO nanowire growth was investigated by comparing the performances of Au, Pt, and Ag nanoparticles. Additional control of growth was achieved by implementing a substrate temperature of either 800 °C with a ZnO/graphite powder source or 500 °C with a Zn powder source. At 800 °C, the vapor−liquid−solid mechanism plays a very important role when the Au and Pt nanoparticles are in the liquid phase. On the other hand, nanowires can also be grown on solid nanoparticles, that is, oxidized Ag at 800 °C and nanoscale cracks, that is, Pt at 500 °C, where, the vapor−solid is the only possible mechanism. At 500 °C, the vapor−liquid mechanism still dominates even though Au and Ag appear to be liquid, which is a result of high Zn vapor pressure.

Introduction

ZnO is one of the most important (opto-) electronic materials with a wide and direct band gap of 3.37 eV and a large exciton binding energy of 60 meV at room temperature. Recently, there has been a lot of interest in growing ZnO nanostructures, especially nanowires and nanorods, motivated by their remarkable physical and chemical properties and the potential applications as nanoscale electronic, photonic, field emission, sensing, and energy conversion devices.[1−8] Several strategies have been developed to synthesize ZnO nanowires and nanorods, such as vapor-phase transport,[1,9,10] metalorganic vapor-phase epitaxy,[11] pulsed laser deposition,[12] and various wet-chemistry methods.[13]

In the popular vapor transport method the ZnO nanowire growth usually takes place on silicon, sapphire, or nitride substrates coated with Au catalytic nanoparticles.[14,15] In most cases, the vapor−liquid−solid (VLS) process was claimed as the growth mechanism. VLS was first proposed by Wagner and Ellis for silicon whisker growth.[16] In general, for the VLS growth, it is important to choose an appropriate catalyst and synthesis temperature so that there is a coexistence of liquid alloy and solid nanowire material.[17] The growth material is evaporated first, and then it forms a eutectic liquid alloy with the catalytic nanoparticles. The ensuing supersaturation leads to the precipitation and the growth of nanowires at the interface between the substrate and the liquid nanoparticles. In this mechanism, the catalytic particles direct the growth direction and normally stay at the growth front, that is, the top of the nanowires.

On the other hand, it is frequently observed that ZnO nanowires can also be synthesized without any catalyst,[18−21] following most likely the vapor−solid (VS) process.[22,23] Such an anisotropic growth could be the result of several factors, such as, different growth rates of different crystal orientations, existence of dislocations, or preferential accumulation of impurities on certain facets. For ZnO, the growth speed is crystallographic-direction-dependent with the [001] direction much faster than [100] and [210]. Due to the constraints that originated from liquid-phase catalyst nanoparticles, beyond one-dimensional nanowires and nanorods, the VLS process seldom leads to the formation of complex structures. In general, the VS mechanism is the driving force behind the synthesis of many kinds of ZnO architectures and hierarchical nanostructures, such as tetrapods,[24] nanotubes,[25,26] nanoneedles,[27] nanohelices and nanosprings,[28] nanorings,[29] nanodisks,[25,30] nanodonuts,[31] nanobridges and nanonails,[32] nanopins,[33] nanocombs,[34] nanowalls,[35] nanoflowers, and so forth.[36]

Under a certain environmental condition it could be controversial how the VLS and the VS mechanisms compete with each other and what roles the catalytic particles play in the growth process. In this report we carried out a systematic study on the growth mechanism by tuning two important parameters: Zn vapor pressure and catalyst. First, we adjusted the Zn vapor pressure by using either ZnO/graphite or Zn powder as the source material. ZnO has a very high melting point of 1975 °C, and its reduction to Zn vapor is impossible without graphite. Compared with the ZnO/graphite source, the Zn powder was observed to generate a much higher vapor pressure. As we will demonstrate, adjusting the Zn vapor pressure is an effective tool to control the nanowire growth mechanism. Second, we could gain more insight on the growth-related issues

* Author to whom correspondence should be addressed. E-mail: tomwu@ntu.edu.sg.

10.1021/jp075296a CCC: $37.00
Published on Web 11/03/2007

by synthesizing ZnO nanowires using different catalysts. Catalyst metal selection is of vital importance to achieve the desired nanowire morphology and to avoid any potential detrimental contamination.[37] Recently, 15 metal catalysts of periods IV, V, and VI were used to grow tin oxide nanowires, and their performances were compared.[37] For ZnO nanowire growth, besides Au, there have been reports on using Sn, Ni, Cu, and Se as the catalysts.[38−42] We purposefully chose Au, Pt, and Ag because that they are physically active, but chemically inert. This report is the first study on using Pt and Ag as catalysts to grow ZnO nanowires. We found that both Pt and Au remain inert at all temperatures used in our experiments, while Ag oxidizes quickly above 500 °C. The state of the nanoparticles is of vital importance in determining the growth mechanisms, since the existence of liquid metal droplets is a prerequisite for the VLS process to occur. Indeed, liquid-state Au and Pt nanoparticles lead to the VLS growth of ZnO nanowires at 800 °C. However, we found that at 500 °C the VS process plays a dominating role even when the liquid-phase catalytic nanoparticles are present. In general, there exists a dynamic competition between the VLS and the VS mechanisms, and the winner is determined by subtle changes of experimental conditions.

Experimental Section

In our experiments, we used either ground ZnO and graphite powders with a weight ratio of 1:1 or Zn powder as the source material. The growth setup consists of a horizontal three-zone tube furnace, a rotary pump, and a gas delivery system. The alumina furnace tube has a diameter of 6 cm. A small one-end-open quartz tube with a diameter of 1 cm containing the source was put near the middle of the tube furnace. Silicon substrates were sputtered with 3 nm films of either Au, Pt, or Ag before being put a few centimeters downstream from the source. After being pumped down to a few millitorrs, the furnace was heated quickly to either 1100 °C for the ZnO/ graphite source or 500 °C for the Zn source and held for an hour before cooling to room temperature. Argon gas with a trace amount (0.05%) of oxygen was used as the carrier gas with a flow of 100 sccm. The temperature of the substrates was measured to be ~800 °C for the ZnO/graphite case and ~500 °C for the Zn case. A JEOL JSM-6700 F field emission scanning electron microscope (SEM) and a high-resolution transmission electron microscope (TEM, JEOL 2100) were used to study the nanowire morphology and structure. The composition was determined by an energy-dispersive spectrometer (EDX) attached to the TEM. The structural analysis was carried out using a Bruker AXS D8 Advanced powder diffractometer with Cu Kα radiation.

Results and Discussion

Figure 1 shows top and perspective views of the nanowires, whose diameters are 46.5 ± 11.7, 111.9 ± 52.0, and 90.3 ± 36.1 nm for the Au, Pt, and Ag cases, respectively. Au nanoparticles result in the thinnest and longest nanowires. In order to obtain some information on the growth speed, we terminated the growth immediately after ramping to the highest temperature and found that the nanowires are already 0.4 μm long. The average nanowire length is 0.6 and 1.5 μm after growth times of 1 and 3 min, respectively. Therefore the growth speed is approximately 10 nm/s at the initial stage of growth and then decreases as the source powder runs out. Nanowires grown on Ag nanoparticles are much shorter than for the other two cases. For all samples, X-ray diffraction (XRD) peaks

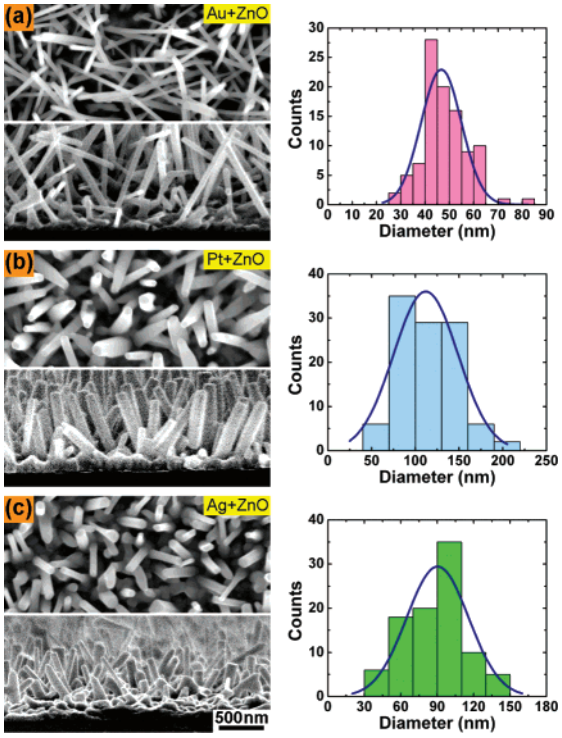

Figure 1. SEM top and perspective views of nanowires grown from a ZnO/graphite source at 800 °C on (a) Au, (b) Pt, and (c) Ag nanoparticles. Their histograms of size distribution are shown on the right side.

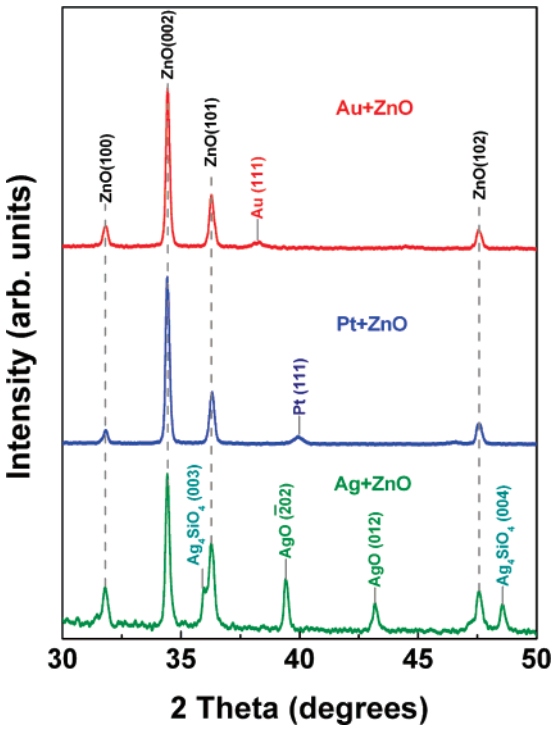

Figure 2. XRD patterns of three nanowire samples grown on Au, Pt, and Ag nanoparticles.

related to ZnO shown in Figure 2 can be indexed as the wurtzite structure (a = 3.25 Å and c = 5.21 Å). Only Au and Pt peaks are identified in the XRD data, indicating that they remain inert during annealing, consistent with previous studies.[43] However, we found that Ag forms compounds of Ag_4SiO_4 and AgO.

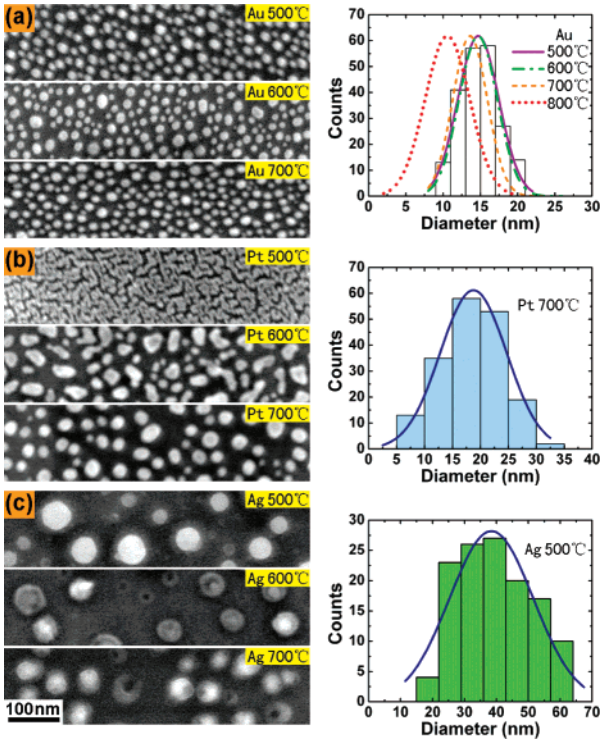

Figure 3. SEM images of (a) Au, (b) Pt, and (c) Ag nanoparticles annealed at different temperatures. Histograms of size distribution for Au at annealing temperatures from 500 to 800 °C, for Pt at 700 °C, and for Ag at 500 °C are shown on the right side.

In control experiments we patterned the metal films before annealing and found that nanowires grow only in areas coated with nanoparticles, not on a bare silicon surface. Although catalytic nanoparticles are of vital importance for the growth of a wide rang of nanowires, their state and kinetics remain controversial.[44] To study the morphological evolution of the nanoparticles and their roles in the nanowire growth, 4 nm sputtered films of Au, Pt, and Ag are annealed at different temperatures for ~30 min without nanowire growth. In all three cases, liquid-droplet-like nanoparticles emerge at temperatures well below their bulk melting points, which are 1064, 1772, and 962 °C for Au, Pt, and Ag, respectively. Such significant size-dependent reductions of melting points have been reported to be in excess of that predicted by the Gibbs−Thompson theory.[45] As shown in Figure 3, the Au film forms nanoparticles with homogeneous size distributions at all annealing temperatures, concurring with the prevalent usage of Au as catalyst for nanowire growth. The nanoparticle diameters are 14.7 ± 3.9, 14.8 ± 3.6, 13.7 ± 3.3, and 10.6 ± 4.2 nm at 500, 600, 700, and 800 °C, respectively. The smaller particle sizes at 700 and 800 °C could be a result of their more spherical shapes at these higher temperatures. At 500 °C the Pt film does not form nanoparticles, but shows very fine cracks instead. Particles with irregular shapes emerge at 600 °C as a result of enhanced but still limited mobility. Circular Pt particles with a diameter of 18.7 ± 8.4 nm eventually form at 700 °C. Ag forms circular particles at 500 °C with a size distribution of 38.4 ± 18.5 nm, much larger than the previous two cases, suggesting stronger agglomeration. Oxidation of Ag nanoparticles starts and accelerates at 600 and 700 °C, reflected by the strong charging effect in the SEM images, which is consistent with the XRD results. Ag nanoparticles after oxidation do not change much in size and shape as annealing temperature increases, suggesting that they are in the solid phase. For all three cases, future high-temperature XRD studies are planned to investigate in detail the solid−liquid transitions and to determine the optimal temperature for nanowire growth. As shown in Figure 1, nanowires grow at ~800 °C in all three cases including Ag. Therefore, we can conclude that liquid droplets are not a prerequisite for the nanowire growth, although Figure 1 suggests that liquid nanodroplets (Au and Pt) result in nanowires with a better quality, that is, longer and more uniform, than the solid counterpart (Ag).

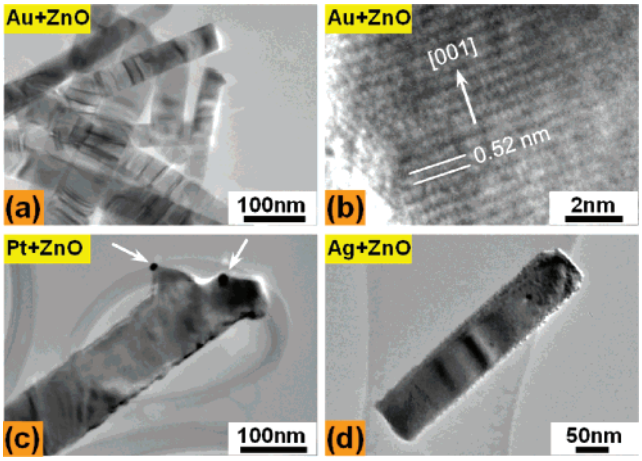

Figure 4. TEM images of ZnO nanowires grown from a ZnO/graphite source at 800 °C on (a, b) Au, (c) Pt, and (d) Ag nanoparticles.

TEM data in Figure 4 show that for the Ag and Au cases there is no metal or alloy nanoparticle on the ends of nanowires. It is not surprising for Ag because it is already oxidized into solid particles before the nanowire growth starts. However, for Au, several groups were observed terminating Au catalytic nanoparticles, which is generally considered as an indicator for the VLS growth.[7,14,34] The absence of nanoparticles in our case could be a result of enhanced evaporation or migration of Au under the particular environmental conditions used in our experiments. Recently, some studies have suggested that the morphological evolution of Au catalyst and its role in the nanowire growth process are much more complex than a conventional VLS picture. A recent TEM study showed that Au exhibits high mobility and can migrate along the silicon nanowires.[46] The depletion of Au from the growth fronts, that is, the nanowire tops, eventually terminates the nanowire growth. Another study showed that Au resides around the base of ZnO nanowires instead of at the top.[47] It was claimed that the VS mechanism controls the nanowire growth although the VLS mechanism is responsible for the formation of [0001]-oriented ZnO nuclei at the initial stage. However, for two reasons, we believe that VLS still is the dominating mechanism for the growth at 800 °C with Au and Pt catalysts. First, for the Pt case we observed multiple tiny nanoparticles at the nanowire ends, highlighted by arrows in Figure 4c and identified as Pt by EDX. It corroborates the scenario that the nanoparticles remain in liquid form with high mobility and migrate or evaporate away from the nanowires during the growth process, similar to previous studies.[42,46] Such an annihilation effect could be weaker and slower in the Pt case than in the Au case, leaving out tiny Pt nanoparticles. Second, a high vapor pressure is required for the VS mechanism to occur. The Zn vapor from the ZnO/graphite powder source is much less than from the Zn powder source. The large diameter of the furnace tube further reduces the effective supersaturation of Zn vapor. Under such experimental conditions the VS process could only result in

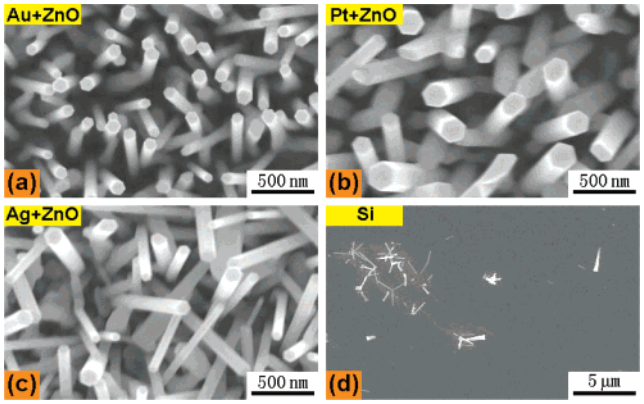

Figure 5. SEM images of ZnO nanowires grown from a Zn source at 500 °C on (a) Au, (b) Pt, and (c) Ag. (d) Sparse nanowires grow around scratches on a bare silicon substrate.

nanowires with much lower quality, namely, shorter length and inhomogeneous diameter distribution. That is the case for Ag, where VS is the only mechanism as a result of the absence of liquid-state catalyst. Therefore, for the cases of Au and Pt, we believe that the VLS mechanism plays a very important role although the VS mechanism might take over after the metal nanoparticles are depleted from the growth fronts.

Since Pt does not form nanoparticles at 500 °C, we can assess the importance of nanoparticle morphology for the nanowire growth by conducting experiments at this particular temperature. Both Zn powder and silicon substrates are heated to 500 °C with other experimental conditions kept the same. As shown in Figure 5, thick nanowires with flat hexagonal tops are grown for all three cases. For the case of Ag, ZnO nanowires grow much better at 500 °C than at 800 °C, which could be a result of less oxidation. Since Pt nanoparticles do not form at 500 °C, from Figure 5b we can conclude that nanoparticle morphology is not a prerequisite for nanowire growth. On the other hand, the nanoscale cracks in the 500 °C annealed Pt film shown in Figure 3b serve as nucleation sites for the Zn vapor absorption. As shown in Figure 5d, nanowires do not grow on bare silicon substrates, but on some defective structures such as scratches. Certainly the nanoscale regular cracks on the 500 °C annealed Pt films provide much better nucleation sites for the nanowire growth, leading to high-density growth and homogeneous size distribution. Similarly, high-quality ZnO nanowires were previously grown on other surfaces with microcurvatures such as carbon cloth.[48] We also note that at 500 °C Pt does not form liquid droplets with Zn vapor. Otherwise, alloy particles similar to the 800 °C case would have been observed at the ends of nanowires due to the lower mobility of Pt atoms at 500 °C. Since no liquid-phase nanoparticle is involved in the Pt case, the nanowire growth has to follow the VS route.

At 500 °C, Au and Ag already form liquid-phase droplets and start trapping Zn vapor with high accommodation efficiency. However, we argue that the VS mechanism still plays a much more important role than the VLS mechanism on the basis of the following two observations. First, compared with the 800 °C growth, evaporation and migration of catalysts should be much weaker due to the lower temperature. The fact that all the nanowires show smooth flat hexagonal tops regardless of catalyst types suggests that the VLS mechanism cannot play the dominating role in this low-temperature growth. Otherwise we should have seen the remains of catalysts at the end of nanowires. The well-defined hexagonal column shape of the nanowires also suggests the anisotropic growth and the VS mechanism. Second, in this set of experiments the supersaturation pressure of the Zn vapor is much higher than the previous one, which may affect the competition between VLS and VS growth. The impingement rate on the nanowire ends, W, is given by

$$W = \pi r^2 p\left(\frac{m}{2\pi kT}\right)^{(1/2)}$$

where r is the nanowire radius, p is the Zn vapor pressure, m is the mass of the Zn atom, k is the molecular gas constant, and T is the absolute temperature of the vapor phase.[22] Therefore, a higher vapor pressure increases the growth rate and promotes the VS growth. The Zn powder source produces a much higher vapor pressure than the ZnO/graphite powder source. In our experiments, we routinely observed that the pressure inside the furnace tube rapidly increases after the Zn source is heated to 450 °C. On the other hand, we did not notice such dramatic variations of pressure when using the ZnO/graphite powder source. Although in the Au and Ag cases, the strong nonequilibrium conditions may even trigger both VLS and VS growth simultaneously,[47] the high vapor pressure associated with the Zn powder source may favor the VS mechanism in general. When we increased the growth temperature higher than 500 °C, nanocombs frequently appeared, suggesting a more violent VS growth. Certainly, further studies are imperative to assess the individual contributions from the VLS and VS mechanisms if other experimental variables, such as gas flow rate, gas pressure inside the furnace tube, source temperature, and so forth are changed.

In general, compared with the VS mechanism, the VLS mechanism enforces much more strict requirements on the experimental conditions and the catalysts used. In our experiments the liquid-state nanoparticles of Au and Ag at 500 °C did not lead to the VLS growth, likely due to the low mobility of Au and Ag atoms. The Zn vapor may not form alloys with Au and Ag or condense out near the substrate to form ZnO nanowires with oxygen. In other words, Au and Ag nanoparticles merely serve as nucleation sites, trapping Zn vapor, similar to the role played by the Pt film with nanocracks. A recent study on InAs nanowire growth also suggested that the VLS mechanism does not apply and Au particles merely provide a low-energy interface to collect precursor materials.[49] Compared with conventional VLS processes, ZnO nanowire growth is unique due to the existence of oxide in addition to metals and alloys. Furthermore, with the exception of the Sn−Zn and In−Zn combinations, the phase diagrams of Zn alloying with many metals are much more complex than those involving conventional semiconductors.[17] The "V"-shaped phase diagrams of Au−Si, Fe−Si, and Au−GaAs have been used to predict the formation of nanowires within certain ranges of temperature, which were verified by experiments.[17] However, the absence of a pronounced "V" shape in most phase diagrams of Zn alloys indicates a different growth mechanism. Therefore, the oxide formation must play a critical role and requires further fundamental studies. Compared with non-oxide semiconductors, ZnO nanowire growth appears to be more subtle and many details remain unclear.

Recently, several groups have reported on a self-catalyzed growth,[50,51] namely, Zn liquid droplets condensing and acting as a catalyst for the ensuing nanowire growth. Such self-catalyzed growth involves liquid droplets, but not external catalysts. Therefore, it is different from the conventional VLS growth. In many aspects, such a self-catalyzed growth resembles

TABLE 1: Summary of Experimental Conditions, Catalyst States, and Growth Mechanisms of Nanowires

	source					
	mixed ZnO/ graphite powder			Zn powder		
substrate temperature	800 °C	800 °C	800 °C	500 °C	500 °C	500 °C
Zn vapor pressure	low	low	low	high	high	high
catalyst material	Au	Pt	Ag	Au	Pt	Ag
state of catalyst	liquid	liquid	solid	liquid	solid	liquid
growth mechanism	VLS	VLS	VS	VS	VS	VS

the VS process except the existence of liquid Zn droplets at the nanowire ends during the growth. However, this mechanism may not be dominant in our case. In the self-catalyzed mechanism, sharp tips were found at the ends of nanowires as a result of condensation from a liquid phase.[51] However, in our experiments, all the nanowires grown at 500 °C show smooth flat tops. Furthermore, the self-catalyzed mechanism enables growth on bare Si substrates.[51] On the contrary, we saw few nanowires on bare substrates or areas not covered by catalysts. Therefore, although the substrate temperature (500 °C) is higher than the melting temperature of Zn (419 °C), upon absorption Zn vapor immediately forms ZnO with oxygen and no liquid Zn droplet is formed.

Conclusion

Table 1 summarizes the experimental conditions we used as well as the proposed growth mechanisms for each case. We found that the Zn powder source produces a very high vapor pressure, facilitating the VS growth regardless of what catalytic particles are used. In our experiments, Pt and Ag nanoparticles were used to grow ZnO nanowires for the first time and their performances are compared with Au. The thinnest and longest nanowires are grown on Au, facilitated by the homogeneous nanoparticles formed in a wide range of temperatures. Ag nanoparticles are effective for growing nanowires at 500 °C. But at higher temperatures Ag oxidizes quickly, resulting in low-quality nanowires. The Pt film forms cracks at 500 °C, but nanowires can still grow via the VS mechanism.

The presence of catalytic nanoparticles is critical for nanowire growth although neither liquid-phase droplets nor nanoparticle morphology is a prerequisite. In our control experiments, very few nanowires grow on smooth bare silicon substrates no matter what source or catalyst we used. Selecting catalytical nanoparticles and source materials appears to be an effective approach to adjust the competition between the VLS and the VS mechanisms and to tailor the growth of ZnO nanowires with desired morphologies and properties. For the VLS process, nanoscale liquid droplets are indispensable due to their ability to effectively absorb and form alloys with Zn vapor. On the other hand, for the VS growth, which dominates in most situations, these nanoparticles mainly provide nanoscale nucleation sites. High-quality ZnO nanowires should grow with many other catalysts under the conditions that these catalysts form nanoparticles with a homogeneous size distribution and that they do not oxidize under the growth environment. More detailed investigations related to catalysts are imperative to grow nanowires with controlled morphology and to dope nanowires with active elements to achieve desired functionalities. The methodology elaborated here should be applicable to these future endeavors on nanowire growth. Further studies using, for example, in-situ TEM are required to achieve detailed structural and chemical information on the interactions between catalysts and nanowires as well as a better control of growth kinetics, orientation, and morphology.

Acknowledgment. The authors acknowledge Research Grant SUG 20/06 and Institute of Materials Research and Engineering for support.

References and Notes

(1) Huang, M. H.; Mao, S.; Feick, H.; Yan, H.; Wu, Y.; Kind, H.; Weber, E.; Russo, R.; Yang, P. *Science* **2001**, *292*, 1897.
(2) Wang, Z. L. *J. Phys.: Condens. Matter* **2004**, *16*, R829.
(3) Ng, H. T.; Han, J.; Yamada, T.; Nguyen, P.; Chen, Y. P.; Meyyappan, M. *Nano Lett.* **2004**, *4*, 1247.
(4) Heo, Y. W.; Tien, L. C.; Kwon, Y.; Norton, D. P.; Pearton, S. J.; Kang, B. S.; Ren, F. *Appl. Phys. Lett.* **2004**, *85*, 2274.
(5) Park, W. I.; Kim, J. S.; Yi, G.-C.; Bae, M. H.; Lee, H.-J. *Appl. Phys. Lett.* **2004**, *85*, 5052.
(6) Li, Q. H.; Liang, Y. X.; Wan, Q.; Wang, T. H. *Appl. Phys. Lett.* **2004**, *85*, 6389.
(7) Chang, P.-C.; Fan, Z. Y.; Chien, C.-J.; Stichtenoth, D.; Ronning, C.; Lu, J. G. *Appl. Phys. Lett.* **2006**, *89*, 133113.
(8) Wang, X. D.; Song, J. H.; Liu, J.; Wang, Z. L. *Science* **2007**, *316*, 102.
(9) Pan, Z. W.; Dai, Z. R.; Wang, Z. L. *Science* **2001**, *291*, 1947.
(10) Wu, J.-J.; Liu, S.-C. *Adv. Mater.* **2002**, *14*, 215.
(11) Park, W. I.; Kim, D. H.; Jung, S.-W.; Yi, G.-C. *Appl. Phys. Lett.* **2002**, *80*, 4232.
(12) Hartanto, A. B.; Ning, X.; Nakata, Y.; Okada, T. *Appl. Phys. A* **2004**, *78*, 299.
(13) Vayssieres, L.; Keis, K.; Lindquist, S. E.; Hagfeldt, A. *J. Phys. Chem. B* **2001**, *105*, 3350.
(14) Yang, P.; Yan, H.; Mao, S.; Russo, R.; Johnson, J.; Saykally, R.; Morris, N.; Pham, J.; He, R.; Choi, H.-J. *Adv. Funct. Mater.* **2002**, *12*, 323.
(15) Wang, X. D.; Song, J. H.; Li, P.; Ryou, J. H.; Dupuis, R. D.; Summers, C. J.; Wang, Z. L. *J. Am. Chem. Soc.* **2005**, *127*, 7920.
(16) Wager, R. S.; Ellis, W. C. *Appl. Phys. Lett.* **1964**, *4*, 89.
(17) Hu, J. T.; Odom, T. W.; Lieber, C. M. *Acc. Chem. Res.* **1999**, *32*, 435.
(18) Tseng, Y.-K.; Huang, C.-J.; Cheng, H.-M.; Lin, I.-N.; Liu, K.-S.; Chen, I.-C. *Adv. Funct. Mater.* **2003**, *13*, 811.
(19) Ye, C. H.; Fang, C. S.; Hao, Y. F.; Teng, X. M.; Zhang, L. D. *J. Phys. Chem. B* **2005**, *109*, 19758.
(20) Yang, Y. H.; Wang, C. X.; Wang, B.; Li, Z. Y.; Chen, J.; Chen, D. H.; Xu, N. S.; Yang, G. W.; Xu, J. B. *Appl. Phys. Lett.* **2005**, *87*, 183109.
(21) Sekar, A.; Kim, S. H.; Umar, A.; Hahn, Y. B. *J. Cryst. Growth* **2005**, *277*, 471.
(22) Sears, G. W. *Acta Metal.* **1955**, *3*, 361.
(23) Sears, G. W. *Acta Metal.* **1955**, *3*, 367.
(24) Yan, H.; He, R.; Pham, J.; Yang, P. *Adv. Mater.* **2003**, *15*, 402.
(25) Gao, P. X.; Lao, C. S.; Ding, Y.; Wang, Z. L. *Adv. Funct. Mater.* **2006**, *16*, 53.
(26) Mensah, S. L.; Kayastha, V. K.; Ivanov, I. N.; Geohegan, D. B.; Yap, Y. K. *Appl. Phys. Lett.* **2007**, *90*, 113108.
(27) Zhu, Y. W.; Zhang, H. Z.; Sun, X. C.; Feng, S. Q.; Xu, J.; Zhao, Q.; Xiang, B.; Wang, R. M.; Yu, D. P. *Appl. Phys. Lett.* **2003**, *83*, 144.
(28) Gao, P. X.; Ding, Y.; Mai, W.; Hughes, W. L.; Lao, C.; Wang, Z. L. *Science* **2005**, *309*, 1700.
(29) Kong, X. Y.; Wang, Z. L. *Nano Lett.* **2003**, *3*, 1625.
(30) Xu, C. X.; Sun, X. W.; Dong, Z. L.; Yu, M. B. *Appl. Phys. Lett.* **2004**, *85*, 3878.
(31) Chao, L. C.; Chiang, P. C.; Yang, S. H.; Huang, J. W.; Liau, C. C.; Chen, J. S.; Su, C. Y. *Appl. Phys. Lett.* **2006**, *88*, 251111.
(32) Lao, J. Y.; Huang, J. Y.; Wang, D. Z.; Ren, Z. F. *Nano Lett.* **2003**, *3*, 235.
(33) Xu, C. X.; Sun, X. W. *Appl. Phys. Lett.* **2003**, *83*, 3806.
(34) Chen, Y. X.; Lewis, M.; Zhou, W. L. *J. Cryst. Growth* **2005**, *282*, 85.
(35) Ng, H. T.; Li, J.; Smith, M. K.; Nguyen, P.; Cassell, A.; Han, J.; Meyyappan, M. *Science* **2003**, *300*, 1249.

(36) Shen, G. Z.; Bando, Y.; Chen, D.; Liu, B. D.; Zhi, C. Y.; Golberg, D. *J. Phys. Chem. B* **2006**, *110*, 3973.
(37) Nguyen, P.; Ng, H. T.; Meyyappan, M. *Adv. Mater.* **2005**, *17*, 1773.
(38) Gao, P. X.; Ding, Y.; Wang, Z. L. *Nano Lett.* **2003**, *3*, 1315.
(39) Li, S. Y.; Lee, C. Y.; Tseng, T. Y. *J. Cryst. Growth* **2003**, *247*, 357.
(40) Xu, C. X.; Sun, X. W. *Appl. Phys. Lett.* **2003**, *83*, 3806.
(41) Kong, Y. C.; Yu, D. P.; Zhang, B.; Fang, W.; Feng, S. Q. *Appl. Phys. Lett.* **2001**, *78*, 407.
(42) Rybczynski, J.; Banerjee, D.; Kosiorek, A.; Giersig, M.; Ren, Z. F. *Nano Lett.* **2004**, *4*, 2037.
(43) Bootsma, G. A.; Gassen, H. J. *J. Cryst. Growth* **1971**, *10*, 223.
(44) Kodambaka, S.; Tersoff, J.; Reuter, M. C.; Ross, F. M. *Science* **2007**, *316*, 729.
(45) Park, H. D.; Gaillot, A.-C.; Prokes, S. M.; Cammarata, R. C. *J. Cryst. Growth* **2006**, *296*, 159.
(46) Hannon, J. B.; Kodambaka, S.; Ross, F. M.; Tromp, R. M. *Nature (London)* **2006**, *440*, 69.
(47) Fan, H. J.; Lee, W.; Hauschid, R.; Alexe, M.; Rhun, G. L.; Scholz, R.; Dadgar, A.; Nielsch, K.; Kalt, H.; Krost, A.; Zacharias, M.; Gösele, U. *Small* **2006**, *2*, 561.
(48) Banerjee, D.; Jo, S. H.; Ren, Z. F. *Adv. Mater.* **2004**, *16*, 2028.
(49) Dick, K. A.; Deppert, K.; Martensson, T.; Mandl, B.; Samuelson, L.; Seifert, W. *Nano Lett.* **2005**, *5*, 761.
(50) Yao, B. D.; Chan, Y. F.; Wang, N. *Appl. Phys. Lett.* **2002**, *81*, 757.
(51) Geng, C.; Jiang, Y.; Yao, Y.; Meng, X.; Zapien, J. A.; Lee, C. S.; Lifshitz, Y.; Lee, S. T. *Adv. Funct. Mater.* **2004**, *14*, 589.